Characterization of Metal-Doped Methylated Microporous Silica for Molecular Separations

Hany Hassan El-Feky[1], Kelly Briceño[2], Kamila Szałata[1], Miguel A.G. Hevia[3] and Tània Gumí[1,*]

[1]*Departament d' Enginyeria Química, Escola Tècnica Superior d' Enginyeria Química, Universitat Rovira i Virgili, Av. Països Catalans, 26, 43007 Tarragona, Spain*

[2]*Department of Chemical Engineering, Biotechnology and Environmental Technology, University of Southern Denmark, Campusvej 55, 5230 Odense M, Denmark*

[3]*Institute of Chemical Research of Catalonia (ICIQ), Av. Països Catalans, 16, 43007, Tarragona, Spain*

Abstract: Novel silica xerogels are prepared and developed by sol-gel method in the present study. The preparation involves cobalt-doping within the organic templated silica matrices, where methyltriethoxysilane (MTES), which contains methyl groups as a covalently bonded organic template is used. The synthesis and surface properties of cobalt-doped methylated microporous silica xerogels with different MTES and cobalt content are revealed by surface and microstructural techniques, such as TGA, FTIR, X-ray and N_2 adsorption measurements. The doping process enhances the thermal stability of the silica xerogels up to ~ 560 °C in oxidizing atmosphere. Besides, this process has no significant effect on the incorporation of the organic template within the silica matrix. As result of the promoted densification of the xerogels either by increasing MTES content and heat treatment, there is structural change of the silica xerogels such as decreasing the micropore volume and broadening of the pore size distribution. Heat treatment and increasing the cobalt oxide content from 5 to 10% weight ratio resulted in samples with approximately the same structural parameters. This suggests that the cobalt particles are homogeneously dispersed in the silica matrix. The novel silica xerogels exhibit trend toward micropores formation suggesting that these doped silica xerogels can be precursor materials for molecular sieve silica membranes applications. Two silica membranes, hydrophobic and cobalt-doped hydrophobic, are prepared and their performance is examined by the study of transport of He, H_2 and N_2. Preliminary results show that the microporous structure obtained in the unsupported cobalt-doped hydrophobic material are preserved after coating inside the tubular support.

Keywords: Hybrid silica materials, Cobalt-doping, Silica membrane, Hydrophobic membrane, Organic templates.

1. INTRODUCTION

In recent years many strategies have been reported to produce composite membranes for gas separation such as ionic liquids, semi-crystalline polymers (PEA) or mixed matrix membranes (MMM) [1-3]. The need for high thermal stable material for that application is still a topic of growing interest. Microporous silica materials have attracted considerable attention because of their characteristics features as molecular sieving properties. A great demand for those materials impulse the modification of the silica membranes to achieve high performance at high temperature conditions and hydrothermal stability of microporous silica materials is an area of increasing research interest [4-14]. Microporous silica materials with well-controlled physical and chemical properties can be readily synthesized by the sol-gel method involving two main steps: hydrolysis and condensation reactions of the metal alkoxide as described elsewhere [15-17]. The polymeric sol-gel process depends mainly on the control of hydrolysis and condensation reactions. In turn, several studies focused on production of molecular sieving structures with very small pore size distribution in the region of ~ 1 nm or lower. Hence, the sol–gel process is a promising way for obtaining microporous silica materials for gas separation [8, 18-24].

Several attempts of synthesis were designed to prepare unsupported/supported modified silica membranes in order to improve the surface properties of the silica matrix towards molecular sieve applications. One of them consists on template-based approach in which organic templates can be classified as covalently or non-covalently bonded to the siloxane network [25]. In this regard, surface modification using different organic template agents have been reported intensively in the literature [8, 24-32]. Methyltriethoxysilane (MTES), which contains methyl groups as a covalently bonded organic template, is the most common precursor to incorporate organic groups within the oxide network [32]. The tailoring of the silica architectures was achieved via sols prepared using

*Address correspondence to this author at the Departamentd' Enginyeria Química, EscolaTècnica Superior d'Enginyeria Química, Universitat Rovira i Virgili, Av. Països Catalans, 26, 43007 Tarragona, Spain;
Tel: +34 977559617; Fax: +34 977559621; E-mail: tania.gumi@urv.cat

E-ISSN: 2410-1869/15

TEOS and MTES, in absolute ethanol, water, and nitric acid. The organic templates, trapped in the silica matrix, can be burnt off under oxidizing atmosphere[8, 12, 26-28, 33]. Independent of the organic templates used, they show the same behavior at high temperature [26].

The thermal stability of the organic templated silica xerogels, containing MTES, has been studied in both inert and oxidizing atmospheres resulting stable up to 400-500 ^{0}C in both cases [8]. The burnt off can be exploited to generate more micropores, affecting the separation properties of silica membranes as reported by Raman *et al.*[34]. The thermal removal of the organic template hybrid silica depends mainly on the temperature and occurs through continuous condensation reactions that replace the lost of carbon with hydroxyl and siloxane bonds. This leads to continuous microporous network formation as in addition to silica densification originated by the reduction in silanol groups [28, 34]. Incorporating a metal and/or metal oxide in the sol–gel process is other attempt to produce metal-doped molecular sieve silica membrane. For that purpose metal oxides or metal-doped silica sols were prepared through the hydrolysis and condensation of Tetraethylorthosilicate (TEOS) in ethanol and hydrogen peroxide or nitricacid with metal salts, such as hydrated cobalt and nickelnitrate salts or niobium alkoxide. Fine control of the silica matrix and pore size tuning was possible using sol-gel processes [35-38].

Over the last decades, silica materials have been shown to develop promising properties both in terms of permeability and selectivity, particularly towards separation of small kinetic diameter gases such as H_2 [4]. Recently, El-Feky *et al.* reported a novel unsupported silica membrane and the preparation involved cobalt-doping within the matrix of organic templated silica material (hybrid silica) [8]. Such hydrophobic material showed a high thermal stability (up to 500-600 ºC) in both oxidizing and inert atmospheres. Therefore, a novel hydrophobic microporoussilica membrane material, with high thermal stability, have been achieved which can be a precursor material for molecular sieve silica membranes applications. For gas separation applications, especially using tubular membrane module, a tubular or hollow fiber membrane design is considered as a convenient geometry to enhance module packing factor if compared with disk shape membranes [39].

The aim of the present work is to investigate the effect of two parameters: study the characteristics of cobalt-doped organic templated xerogels containing different contents of covalently bonded methyl ligands (MTES) and constant cobalt content (Co: Si weight ratio of 3%). Besides, study the effect of different amounts of cobalt doping in organic templated xerogel matrix with invariant content of covalently bonded methyl ligands (50% TEOS: 50% MTES). Investigation of the heat treatment, especially in oxidizing atmosphere, on the silica matrices was studied as well. For comparison, the temperatures selected in this work are below and above the temperature at which the removal of the organic constituents occur for cobalt-doped hybrid silica (around 560 °C) [8]. Fundamental aspects of the xerogel characterization such as Fourier transform infrared (FTIR), X-ray diffraction, Thermo gravimetric analysis (TGA) as well as the micropore characterization aspects are reported in this study. In order to explore the feasibility of this material in tubular membrane modules for membrane reactors applications, the membranes performance is examined based on the transport analysis of He, H_2 and N_2. The influence of temperature and pressure on membranes permeability and selectivity are studied as well.

2. EXPERIMENTAL SECTION

2.1. Materials and Methods

Tetraethylorthosilicate (TEOS, 98%, Acros Organics), methyltriethoxysilane (MTES, 98%, Acros Organics), ethanol (EtOH, 96% V/V extra pure, Acros Organics), nitric acid (HNO_3, Acros Organics) and cobalt nitrate (99% pure, Acros Organics) were purchased from Scharlab. Distilled water was used for the sols preparation.

2.2. Xerogels Preparation

The silica sols were prepared by the acid-catalyzed hydrolysis and condensation process. Tetraethylorthosilicate (TEOS) and Methyltriethoxysilane (MTES) were used as the silica precursors mixed with ethanol (EtOH), nitric acid (HNO_3), cobalt nitrate (as metal salt) and distilled water as described previously [8]. To avoid the partial hydrolysis during the addition of EtOH to TEOS at room temperature thus, alkoxide/ethanol mixture was placed in ice bath and then acid/water mixture was added drop wise with continuous stirring [32]. For metal doping, a solution of cobalt nitrate in ethanol was used as described previously [8, 40].

Cobalt-doped methyl ligand templated silica xerogels were prepared as follow: after addition of HNO_3/H_2O mixture to TEOS/EtOH mixture. The sol was refluxed under stirring in water bath at 60 ºC for 165 minutes. The reaction mixtures had a (based on starting materials) TEOS: EtOH : H_2O : HNO_3 molar ratio of 1 : 3.8 : 6.4 : 0.085 according to the recipe of the silica sol preparation [41]. Afterwards, mixture of MTES/EtOH solution, which has been placed for 5-10 minutes in ice, and the ethanol solution of the metal salt were added to the reaction mixture and the final sol was refluxed for an additional 15 minutes [8]. The molar ratio of MTES/EtOH solution was X : 3.8, where X = 0.25 - 4, in order to have different mol% of MTES such as 20, 40, 50, 60 and 80 mol%. For instance, for 50% MTES, the mixture had a (based on starting materials) TEOS : MTES : EtOH : H_2O : HNO_3 molar ratio of 1 : 1 : 7.6 : 6.4 : 0.085. In this case the metal salt to metal alkoxide (Co: Si) weight ratio used was 3% for all materials with varying MTES content. The amounts of metal salt were calculated in order to prepare solution of 10% wt/vol of cobalt nitrate in ethanol[8, 40]. Throughout this study the cobalt-doped methyl ligand template silica xerogels are referred to as Co-X% MTES, where X=20, 40, 50, 60 and 80.

For the xerogels with different cobalt content, the metal salt to metal alkoxide (Co: Si) weight ratio used was varied from 3% to 10%. The different cobalt-doped methyl ligand templated silica xerogels are referred to as MTES-X% Co, where X=3, 5, 8 and 10, maintaining the relation 50% TEOS: 50% MTES. All silica sols were allowed to evaporate in Petri-dish at room temperature so that silica flakes, xerogels, were obtained overnight. Xerogels samples were crushed finely to obtain powders, which were used for characterization, and calcined in air at a heating and cooling rate of 1 ºC/min, and held for 3 hours at 400 ºC and 2 hour at 600 ºC.For X-ray comparison of the different xerogels, silica powders were mixed with Co_3O_4 with weight ratio 3%. Cobalt oxide was prepared by calcination of cobalt nitrate in air at 400 ºC.

2.3. Characterization of the Xerogels

Thermogravimetric analysis (thermogravimetry, TGA and differential thermal analysis, DTA) was used to investigate the processes taking place during the heat treatment. This analysis was carried out for dried xerogels in a Thermobalance TGA7 by Perkin Elmer, in synthetic air with a constant flow rate of 290 cm^3 $min^{-1}$and a heating rate of 10 ^0C min^{-1} from room temperature to 900 ºC.

Fourier transform infrared (FTIR) characterization was carried out to determine functional groups within the bulk silica matrix using ATR cell (FTIR 680 Plus JASCO). The absorption spectra were recorded in the 500-1500 cm^{-1} range. The spectrum of each sample represents an average of 32 scans. With the aim of comparison, all FTIR spectra were normalized with respect to the maximum absorbance value for each sample.

XRD for phase detection was conducted using a Siemens D500 diffractometer (Bragg-Brentano parafocusing geometry and vertical θ-θ goniometer). The angular 2θ diffraction range was 5^0 to 70^0. The crystallite size was determined from the line broadening of the diffraction line at $2\theta = 36.8^0$ using the Scherrer equation.

Textural characterization of the synthesized samples was determined by nitrogen adsorption isotherms measurements at -196 ºC in the range $3\times10^{-7} < P/P_0 < 0.995$. The measurements were performed in a Quantachrome Autosorb-iQ adsorption analyzer. Prior to the analysis, the samples were degassed at 250 ºC under vacuum for 12 h. The pore size distribution was calculated from the nitrogen adsorption data using the NLDFT (Non Localized Density Functional Theory) based on a cylindrical pore-equilibrium model.

2.4. Preparation of Supported Hydrophobic Silica Membranes

Two silica membranes, hydrophobic (Hyd-Si) and hydrophobic 3% cobalt-doped silica membrane (Hyd-Co-Si) were prepared. The membranes were coated on inside monochannel γ-Al_2O_3 substrates supported by α-Al_2O_3 (inopor, Germany) with porosity of 3 μm and 5 nm, respectively. The outer and inner diameters of the support are 10 and 7 mm, respectively. The supports were modified and coated several times with the prepared (fresh) sol and then with diluted one, 1: 2 EtOH (3xdilution). The coating processes were performed by using vacuum pump (THOMAS Picolino VTE 3) in order to introduce the sols inside the support channel. After the sol had been introduced, it was kept for an appropriate time inside the support channel; with the purpose to ensure the sol to penetrate in the pores of the support, and therefore modify the intermediate layers of the hydrophobic membranes. These coating processes of the support were repeated four times for each membrane. Finally, the separation layer consisted of the 1: 19 EtOH diluted sol (20x dilution) and this

layer was coated six times. After each coating, either for the intermediate or separation layers, the membranes were calcined in air, for Hyd-Co-Si, or in N_2, for Hyd-Si, at a heating and cooling rate of 1 °C/min, and held for 3 hours at 400 °C. The trend of several coating for intermediate layers preparation and top separation layers was reported by Diniz da Costa *et al.* [18]. The membrane notations throughout the present work are listed in Table **1**.

2.5. Gas Permeance Measurements

Membranes performance was characterized by means of single gas permeation. The tubular hydrophobic membranes were measured in a dead-end mode as depicted in Figure **1**. The set-up for tubular membranes consists of a tubular membrane module and the temperature was controlled with a PID controller. Single gas component permeance measurements were carried out for He, H_2 and N_2 at temperatures ranging from room temperature to 150 °C and pressure differences ranging from 0.5 bar to 3 bar. Ambient moisture can easily condense inside silica micropores, therefore the membranes were dried overnight at 150 °C. All gases were equilibrated for at least half an hour to ensure a constant flow.

3. RESULTS AND DISCUSSION

3.1. Thermogravimetric Analysis

Thermogravimetric analysis was used to investigate the processes occurred during the heat treatment as well as the stability of the organic template (methyl ligands) in oxidizing atmosphere. The weight loss curves of the MTES-X% Co as function of temperature (TGA curve) and the differential weight loss (DTA curve) are shown in Figure **2**. For all samples, also with different MTES content, the initial weight losses from room temperature to ~ 150 °C are mainly attributed to physisorbed water molecules trapped in the silica matrix in addition to the loss of free solvent molecules [26, 28]. The weight loss from ~ 150 to ~ 240 °C is due to the dehydration of cobalt nitrate and the removal of the nitrous gasesand increased as the cobalt content increased [42, 43]. The heat treatment from ~ 240 to ~ 500 °C leads to further condensation reaction, *i.e*. removal of the water and alcohol from the silica matrix [28, 34].

Table 1: Membranes Notations in the Present Study

Membrane Code	Membrane Type	Number of Coating	
		Intermediate Layer	Top Layer
M1	Hyd-Si	4 (N) + 4 (3x)	6 (20x)
M2	Hyd-Co-Si	4 (N) + 4 (3x)	6 (20x)

N: refers to coating with non-diluted sol (fresh prepared sol).

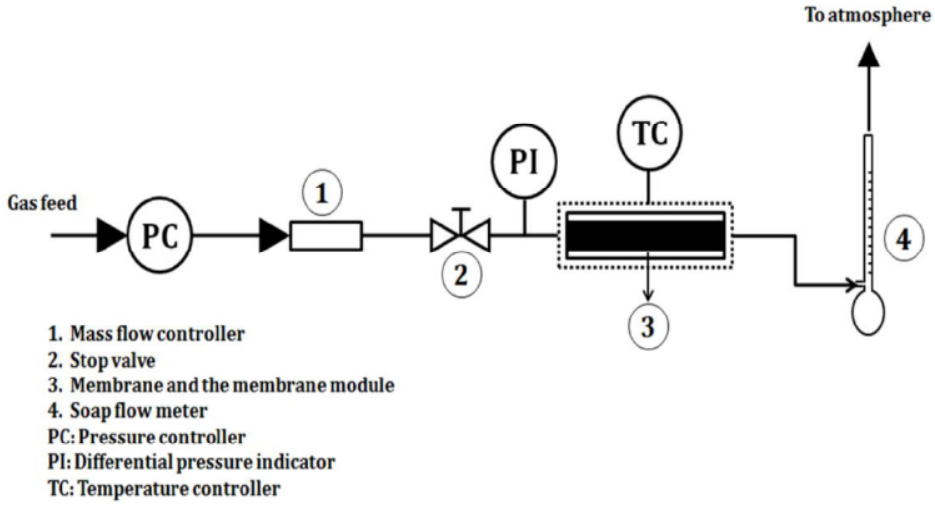

Figure 1: Experimental set-up for dead-end mode for tubular hydrophobic membranes.

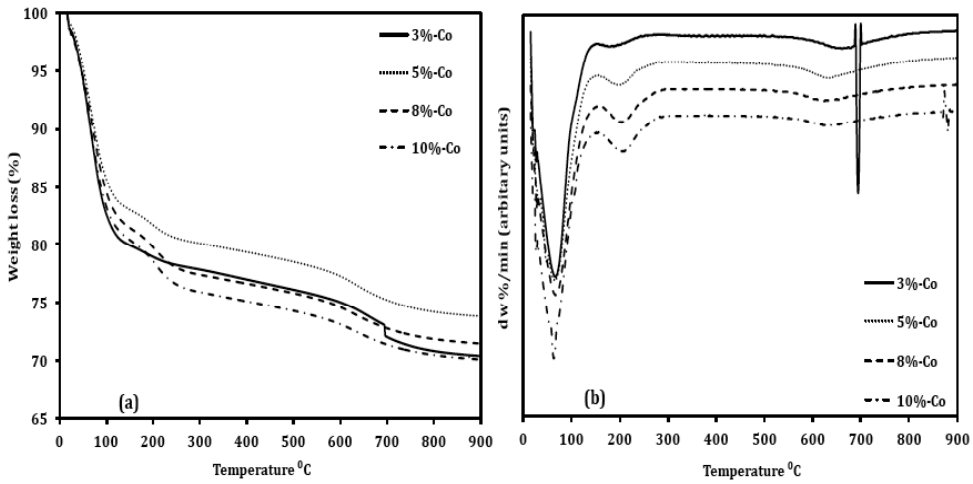

Figure 2: TGA (**a**) and DTA (**b**) of different cobalt content organic templated xerogels.

Table 2: Weight Losses between 500-800 °C of Different Co-X%MTES

% MTES	20	40	50	60	80
Wt loss (%)	2.40	2.56	5.28	5.85	8.12

Recently, metal-doped organic templated silica xerogel, was reported that it is thermally stable in an oxidizing atmosphere up to ~ 560 °C, and more thermally stable than the non-doped one in an inert atmosphere [8].The present study confirm the higher thermal stability in oxidizing atmosphere, regardless the MTES content. This could be related to cobalt composites with silica matrix resulting in the formation of Si-O-Co[8, 44-46]. It has been reported that the weight losses of the organic templated increased with increasing the molar ratio of MTES in the silica matrix and it is also the same case in the present study[28]. Table **2** shows the weight losses of the organic template between 500-800 °C. It can be observed that weight loss increase more than twice when MTES content reach 50%. Thus, molar ratios of sols prepared with MTES: TEOS are generally preferred to be lower.

3.2. Infrared Spectroscopy

Figure **3a** shows the FTIR spectra of dried and calcined Co-50%MTES. Figure **3b** shows the FTIR spectra of MTES-10% Co dried and calcined at 400 and 600 °C (other Co-doped xerogels showed equivalent spectra). The IR bands corresponding to silanol and siloxane bonds appear in the range from ~ 600 to ~ 1450 cm^{-1}, for all samples that were treated at various temperatures. Bands at ~ 770 - 810 cm^{-1} and at ~ 1035 cm^{-1} were assigned to siloxane bonds (Si-O-Si) [6, 8, 47, 48]. Bands at ~ 930 cm^{-1} was assigned to silanol bonds (Si-O-H). This band appears strongly for the dried silica and decrease in intensity after calcination process at 400 and 600 °C. This is in good agreement with what have been reported in the literature [8, 18, 28, 49]. This decrease in intensity is attributed to the polycondensation process which is responsible for the transformation of silanol to siloxane bonds. The band at ~ 1273 cm^{-1} was assigned to asymmetric vibration of the CH_3 group [8, 14, 32, 47, 48]. This band appears strongly for the dried and the calcined sample at 400 °C whereas it is unobservable for MTES-X% Co (with X = 3, 5, 8, 10) and Co-X%MTES samples, where X = 20, 40 and 50,calcined at 600 °C.

Inset graph in Figure **3a** shows the FTIR spectra of Co-60% MTES and Co-80%MTES samples calcined at 600 °C where the band of the CH_3 group is still observable. These results clearly indicate that for Co-X% MTES samples with low MTES content (when X = 20, 40 and 50), most of the organic template (methyl ligands) decomposed or pyrolyzed due to heat treatment in oxidizing atmosphere. According to TGA results around that temperature the decomposition process occurred for all Co-X% MTES samples. Although a high decomposition or pyrolysis processes (high weight losses) occurred as the MTES content increased, when X > 50 mol%, a proportion of the methyl ligands still trapped in the silica matrix. Therefore, the band that was assigned to asymmetric

vibration of the CH_3 group was observed (see inset graph in Figure **3a**).

As the calcination temperature increased, the band at ~ 1035 cm^{-1}, which was assigned to siloxane bonds (Si-O-Si) for the dried samples, shifted with a broad shoulder towards ~ 1040 and 1050 cm^{-1} for Co-X% MTES samples (calcinated at 400 and 600 °C, respectively). For MTES-X% Co samples, the shift occurs from 1022 cm^{-1} to 1035 cm^{-1} for samples calcined at 400 °C, and to 1040 cm^{-1} for samples calcined at 600 °C .This shift is attributed to the change in the xerogel network resulted by the shrinkage in the silica polymeric bonding [8, 48, 49]. Tiny small band at ~ 570 $cm^{-1}$and ~ 670 $cm^{-1}$was assigned to cobalt, in oxide form Co_3O_4; this band appeared after the calcination process whereas this band was no present before the calcination process [6, 8, 45, 50]. As there is no distinguishable peak at ~ 670 $cm^{-1}$for Co-X% MTES these results suggest that the interaction between the methyl ligand templated xerogel matrix and cobalt species depend on the cobalt content as will be mentioned in X-ray section.

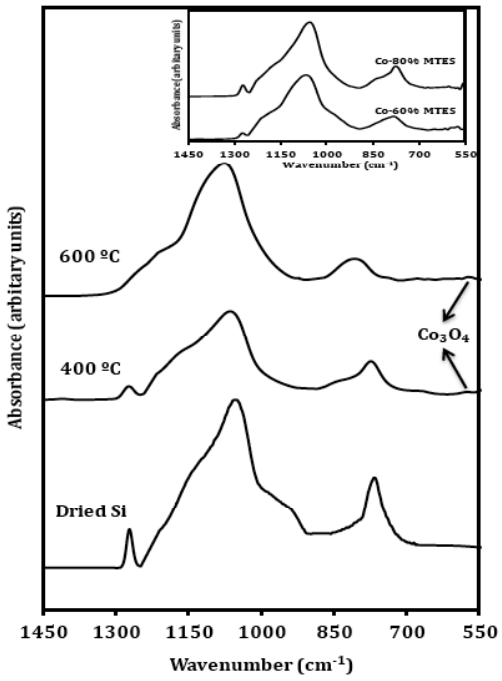

Figure 3a: FTIR spectrum of Co-50% MTES sample.

3.3. X-Ray Analysis

It was reported that as the amount of cobalt content increased,the formation of crystalline Co_3O_4 was obtained. Besides, the treated samples at 400 °C with low cobalt content appeared amorphous[8, 46]. In the present study, the calcined samples with varying MTES

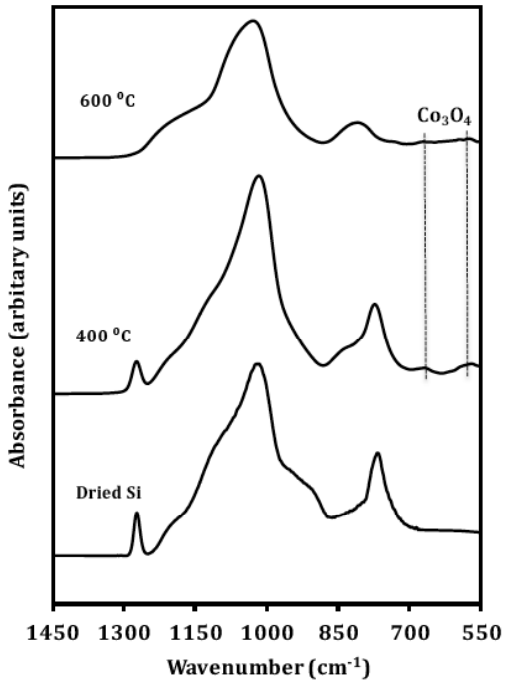

Figure 3b: FTIR spectrum of MTES-10% Co.

content are X-ray amorphous. The results of the calcined MTES-X % Co samples are shown in Figure **4** where it can be seen the difference in their XRD diffractograms which indicates that the nature of the cobalt species and their interaction with the silica matrix strongly depend on both the cobalt content and heat treatment. The result of the MTES-3%Co sample seems amorphous [8], while as the cobalt content increases from 5 to 10%, the peak intensity of (100) for Co_3O_4 (2θ = 36.8^0) increases as well. Moreover, the crystallite size of Co_3O_4 species determined by the Scherrer equation, increases from about 5 nm for 5%-Co to 7 nm for 8%-Co and 8 nm for 10%-Co. Besides, the peak intensity of silica powder with 3% wt. of Co_3O_4 was higher than that of the all different cobalt-doped xerogels.

These results suggest that material with low cobalt content the formation of a mixed matrix of polymeric silica and cobalt oxide particles will be more dominant than the formation of crystalline Co_3O_4. Contrarily, at high cobalt content certain amounts of the cobalt-impregnated in the silica matrix form crystalline Co_3O_4, along with the interaction between the ionic metal as Co^{2+} and the siloxane matrix as reported elsewhere [45]. The formation of Si-O-Co linkage has been postulated to occur through condensation of cobalt oxo-hydroxy complexes $[Co(H_2O)_{6-x-y}(HO)_xO_y]$ with silicone complexes $[Si(OC_2H_5)_{4-n}(OH)_n]$ [45, 46]. Thus, within the silica matrix cobalt can appear in following

forms: ionic metal as Co^{2+}; covalently bound cobalt strongly interacting with the siloxane matrix forming Si-O-Co; tiny Co_3O_4 crystallites that could not be detected by XRD for the low cobalt content sample (3%-Co, and all Co-X%MTES samples) and detectable crystals for the high cobalt content samples, 5-10% Co [8, 35, 45, 46].

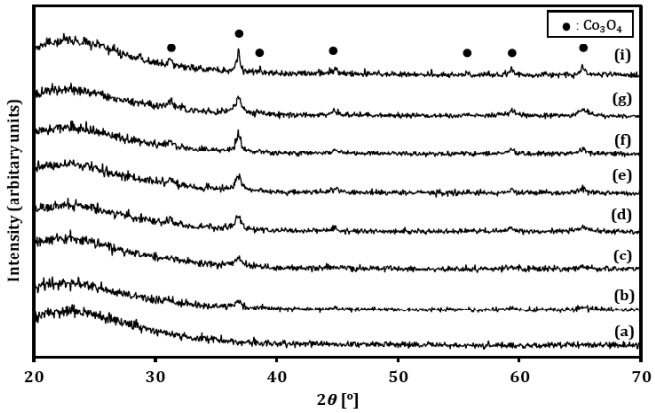

Figure 4: XRD diffractogramms of X%-Co calcined at 400 ^{0}C (**a**) 3%-Co, (**b**) 5%-Co, (**d**) 8%-Co and (**f**) 10%-Co. Samples calcined at 600 ^{0}C (**c**) 5%-Co, (**e**) 8%-Co and (**g**) 10%-Co. (**i**) SiO_2+Co_3O_4 mixture and solid circles represent Co_3O_4 reference pattern.

3.4. Micropore Structure

Textural properties were determined using N_2 adsorption isotherms at -196 ºC. Table **3** represent the parameters obtained from the N_2 adsorption data for the Co-X% MTES samples calcined at 400 °C and 600 °C. Table **4** represent the compilation of structural parameters for the samples MTES-X% Co calcined at 400 °C and 600 °C.The total pore volume, V_T, was obtained from the amount adsorbed at a relative pressure (P/P_0) of 0.99 while the surface area was obtained by application of the BET (Brunauer, Emmett and Teller) method to the nitrogen adsorption data [51]. Micro- and mesoporosity were discriminated using the *t*-plot method [52]. The pore size distributions (PSD) were calculated by applying the NLDFT model to the nitrogen adsorption data at -196 ºC based on a cylindrical pore model [53].

Figure **5a** and **5b** show the N_2 adsorption isotherms for the Co-X% MTES calcined at 400 °C and 600 °C, respectively. In Figure **5a**, all isotherms exhibit the characteristic Type I isotherm with a knee at low relative pressures ($P/P_0 < 0.1$) where occur the majority of pores filling, which is characteristic for microporous

Table 3: Compilation of Structural Parameters Deduced from N_2 Adsorption Data at -196 °C for Co-X% MTES Calcined at 400 °C and at 600 °C

Sample (% MTES)	S_{BET} (m^2g^{-1})		Micropore surface (m^2g^{-1})		$V_{T0.99}$ (cm^3 g^{-1})		V_{micro} (cm^3 g^{-1})	
	400 °C	600 °C	400 °C	600 °C	400 °C	600 °C	400 °C	600 °C
20	563	457	528	418	0.29	0.30	0.25	0.26
40	568	364	526	343	0.36	0.27	0.30	0.23
50	406	320	393	299	0.22	0.22	0.20	0.18
60	471	325	451	303	0.34	0.25	0.30	0.21
80	462	253	432	243	0.37	0.18	0.32	0.16

Table 4: Compilation of Structural Parameters Deduced from N_2 Adsorption data at -196 °C for MTES-X% Co Calcined Samples at 400 °C and 600 °C

Sample (% Co)	S_{BET} (m^2g^{-1})		Micropore Surface (m^2g^{-1})		$V_{T0.99}$ (cm^3 g^{-1})		V_{micro} (cm^3 g^{-1})	
	400 °C	600 °C	400 °C	600 °C	400 °C	600 °C	400 °C	600 °C
3	406	320	393	299	0.22	0.21	0.20	0.18
5	476	351	422	277	0.40	0.27	0.29	0.19
8	484	353	375	275	0.45	0.32	0.23	0.17
10	462	365	372	273	0.42	0.36	0.23	0.17

S_{BET}: Surface area (after application of the Brunauer, Emmett and Teller equation to the nitrogen adsorption data).
$V_{T0.99}$: Total pore volume (from the amount adsorbed at $P/P_0 = 0.95$).
V_{micro}: Micropore volume.

materials [54]. At higher relative pressures ($P/P_0 > 0.4$) the isotherms of samples Co-60% and Co-80% MTES present a positive slope which will most probably correspond to the adsorption in the external area of the samples [55]. The trend is quite clear in the variation in the amount of nitrogen adsorbed which is related to the limiting capacity for each sample. This is mainly dependent on the available micropore volume (rather than the internal surface area) where the interaction between adsorbent and adsorbate occurs. Furthermore, a decrease in the micropore width results in both an increase in the adsorption energy and a decrease in the relative pressure at which the micropore filling occurs (narrow knee in the isotherm) [56]. Apparently, Co-20% and Co-40% MTES samples exhibit a broader knee in the nitrogen isotherm at low relative pressure whereas as the amount of MTES increases, gives rise to a partial blocking/narrowing of the micropores, accompanied by smaller surface area. In fact it is a general trend for organic templated xerogel that the incorporation of organic template results in decreasing the surface area [8, 27, 57].

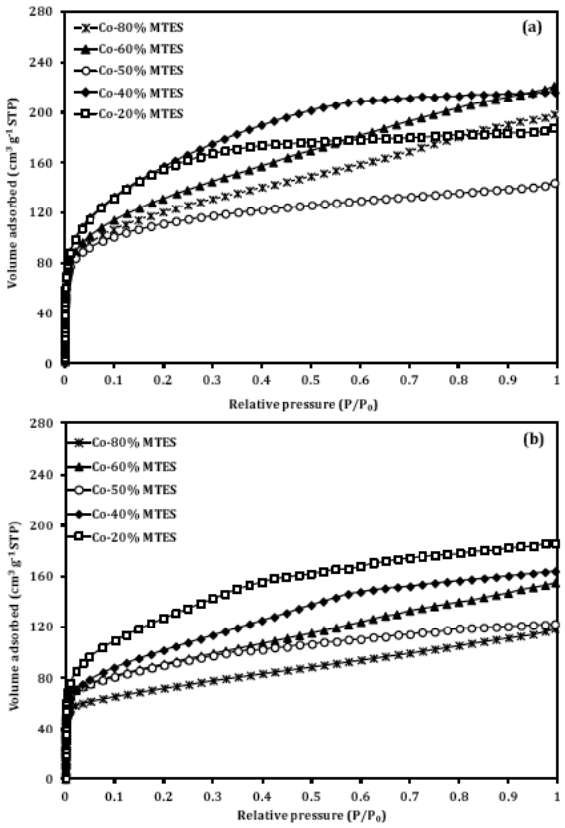

Figure 5: N_2 adsorption isotherms of Co-X%MTES calcined at **a**) 400 °C and **b**) 600 °C.

On the other hand, Figure **5b** shows the N_2 adsorption isotherms Co-X% MTES calcined at 600 °C. At this temperature a high ratio of the decomposition process occurred (see also TGA results). No difference in the isotherm type is observed with regard to the samples calcined at 400 ºC. Raman *et al.* have reported in order to achieve molecular sieve silica membranes by organic template approach, the organic ligands must be uniformly incorporated in the inorganic matrix without aggregation or phase separation to avoid creating pores larger than the size of the individual ligands [34]. It seems that in excess of50% TEOS: 50% MTESmolar ratio occur a non-uniform incorporation of the organic template in the silica matrix. This could be a possible hypothesis for the behavior of the isotherms of samples Co-60% and Co-80% MTES calcined at both temperatures.

Figure **6a** and **6b** represent the N_2 adsorption isotherms for the calcined MTES-X% Co samples at 400 °C and 600 °C respectively, using semilog plots to magnify the micropore adsorption region. The isotherm type, which present a high amount of N_2 adsorbed at low relative pressure and is a behaviour of microporous materials, is the same for samples calcined at these two temperatures[54]. The nitrogen uptake is lower for the samples calcined at 600 ºC. This is due to the higher densification of the silica matrix that occurs at this temperature. As the amount of cobalt increases the isotherms show a slight uptake increase at relative pressure of 0.4 which could be attributed to the presence of crystalline Co_3O_4.Esposito *et al.*confronted the adsorption isotherms of cobalt-doped silica samples with up to 30% mol, obtaining as well large adsorption volumes at $P/P_0 > 0.4$ which increased with cobalt content [45].

Figure **7a** and **7b** show the PSD for the Co-X% MTES calcined at 400 °C and 600 °C, respectively. It can be observed that samples calcined at 400 °C are microporous or bordering the mesoporous region, exhibiting an average pore width between ~ 0.7 and 1.7 nm for Co-20 and Co-40% MTES, between ~ 0.7 and 1.3 nm for Co-50 and Co-60% MTES, and a peak at ~ 1.3 nm for Co-80% MTES. Samples calcined at 600 °C are exhibiting an average pore width between ~ 0.7 and 1.1 nm. This corresponds to the pores filling at low relative pressure leading to a narrow PSD. For Co-X% MTES calcined at 400 °C where X > 50 mol%, peaks over 1 nm broaden, more apparently for Co-80% MTES, which is due to the increasing of the organic template content. This is in good agreement with the PSD results reported in the literature [28, 57]. The peak over 2 nm could be attributed to the fact that silica materials possess wider micropores and mesopores as well. A higher template concentration induce the collapse of the xerogel matrix due to capillary stress

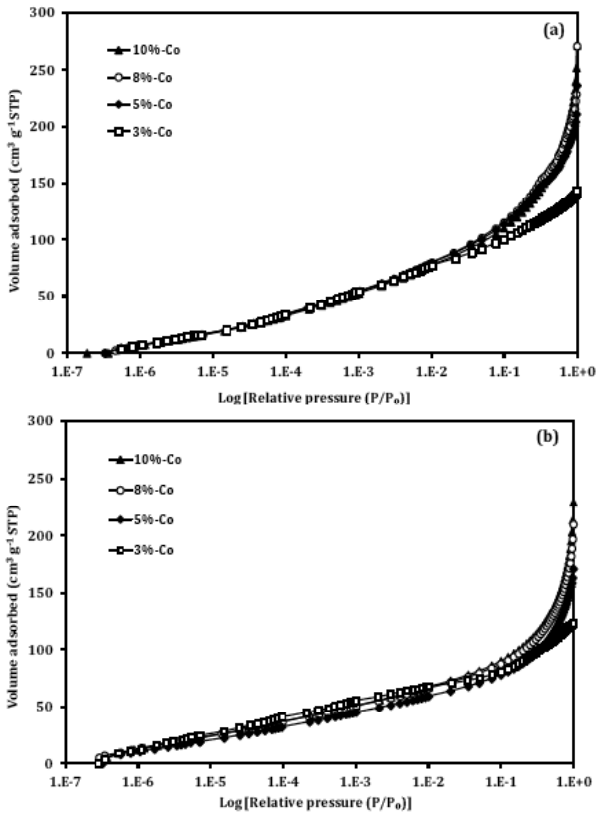

Figure 6: N_2 adsorption isotherms of MTES-X%Co calcined at **a**) 400 °C and **b**) 600 °C.

which promotes dense xerogels and a broader PSD [57]. Figure **8a** and **8b** show the PSD, displayed as semilog plots, of the calcined MTES-X% Co samples at 400 °C and 600 °C, respectively. As it can be noticed all samples are microporous or border the mesoporous region, exhibiting average pore widths at about 0.8 nm, 1.1 nm (more apparently for 3%-Co) and 1.4 nm for samples calcined at 400 °C, and at about 0.8 and 1.1 nm at 600 °C. The supermicroporosity (1,5-2 nm) observed could be attributed to the presence of cobalt in the oxide form as reported elsewhere [45]. However, the PSD results could differ somewhat depending mainly on the model used for the PSD determination

The calcination process provides organic matrix densification due to the reduction in silanol groups and also thereduction in the micropore volume, micropore area and surface area. This process leads to the burnt off the methyl ligands and, as a consequence, continuous condensation reactions replace the lost of carbon with hydroxyl and/or siloxane bonds. This leads to the creation of a continuous microporous network which depends on the uniform incorporation of the organic templates [34]. The structural changes observed in this study are collected in the Table **3** and **4**. The N_2 adsorption isotherms show a knee at low relative pressures ($P/P_0 < 0.1$) which is a characteristic of microporous materials. This indicates that further densification can occur for Co-X% MTES, and hence a continuous network of micropores can be formed even at temperature higher than 550 °C[34]. These changes are observable when comparing the samples calcined at 400 °C and 600 °C. This is quite clear in the PSD curves; Figure **7**, where the peaks over 1.1 nm are not observable for samples calcined at 600 °C as a result of the heat treatment which reduced the micropore volume. Sample Co-20% MTES calcined at 600 °C still showed some peaks over 1.1 nm but with very small height. Thus, it is supported the hypothesis of silica densification because of the heat treatment that leads to a reduction of the pore volume. Those changes in a structure were studied also by Raman *et al.*[34]. In fact, the PSD for Co-80% MTES calcined at 600 °C changed and the heat treatment could be a possible reason of that change. These results indicate that microporous network formation as well as further densification can occur at higher temperature compared with non-doped materials [28, 34]. Such difference is the consequence of the high thermal stability and the organic templates removal at high temperature shown by the material essayed in this work.

In general, as can be seen in Table **3** the micropore area and micropore volume decrease as the MTES content increases, accordingly to the result of Diniz da Costa *et al.* [28] and Fahrenholtz *et al.* [58]. The increase in the MTES content leads to the collapse of the xerogel matrix and promotes denser xerogel formation and lower pore volume [28], which has been attributed to the lower reaction kinetics during gelatin and ageing, and the longer duration of these steps [57]. Non-doped MTES templated silica xerogels showed larger percent of micropore area reduction. For instance, 30 and 40 mol% MTES/TEOS xerogels gave a micropore area reduction of about 57% and 51% by heat treatment from 400 °C to 550 °C and 450 °C to 500 °C respectively. The samples in the present study have higher MTES content, which should lead to a deeper collapse of the silica structure [28]. Nevertheless, they show smaller reduction in the micropore surface area, although the temperature range is higher (from 400 °C to 600 °C).

From the data in Table **4** it can be seen that the difference in cobalt content do not lead to a dramatic change in microporous and total areas and pore volumes. The most different at both calcination temperatures is 3%-Co which has lower BET area and higher micropore area than the other, with the

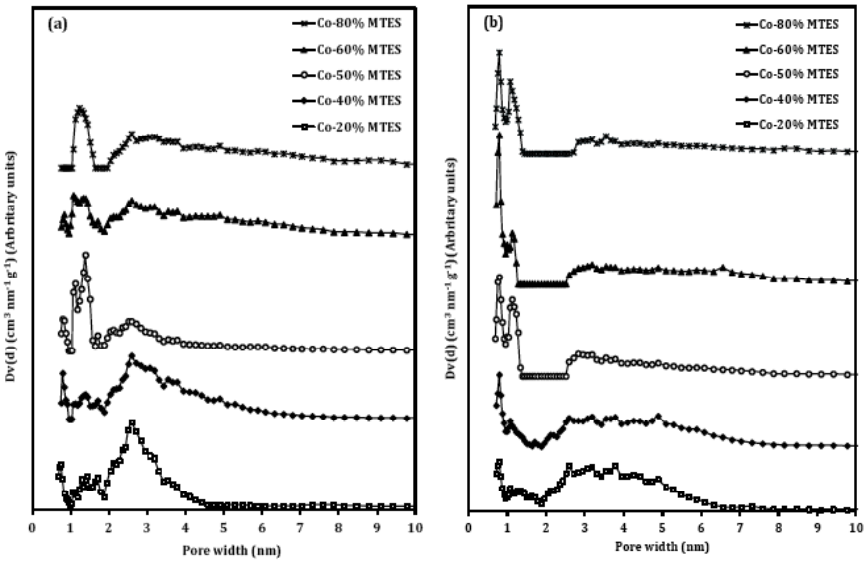

Figure 7: PSD of Co-X%MTES calcined at **a**) 400 °C and **b**) 600 °C.

exception of 5%-Co calcined at 400 ºC that has more micropore area and volume. This could be attributed to the fact that the dominant case for 3%-Co is the formation of the strong framework due to the Si-O-Co linkage, whereas the dominant case for higher cobalt contents is the crystalline structure. In general, due to the metal-doping process, the surface area and micropore volumes should reduce as the metal content increases. Generally the metal content, especially in the oxide form, have low surface area as compared to polymeric silica[45].The obtained results show no significant effect of the amount of doping cobalt at each temperature, despite that the 3%-Co sample deviates from the other samples,*i.e*. has lower BET area and higher micropore area. It suggest that over 3%-Co the cobalt particles, in oxide form, were homogeneously dispersed in the hybrid silica matrix. Similar case have been reported concerning investigation the effect of iron oxide embedded in conventional silica matrices [59]. In addition, this supports that cobalt composite with the silica matrix results in the formation of Si-O-Co linkage for the 3%-Co sample.

The calcination temperature has a larger impact than the cobalt content. The structural changes observed in the samples with different cobalt content are similar to those with varying MTES content. In general, the average of the narrow PSD is still quite constant for the different cobalt contents at each of the calcination temperatures. The biggest change in the micropore surface area exhibits 5%-Co sample, which isfrom 24% after calcination at 400 ºC to 35% at 600 ºC. The similarity of textural parameters among 5-10%-Co samples calcined at 600 ºC indicates that the cobalt-doping process apposed greater collapse of the silica structure and this could be attributed to the homogeneous dispersion of the cobalt oxide within the silica matrix.

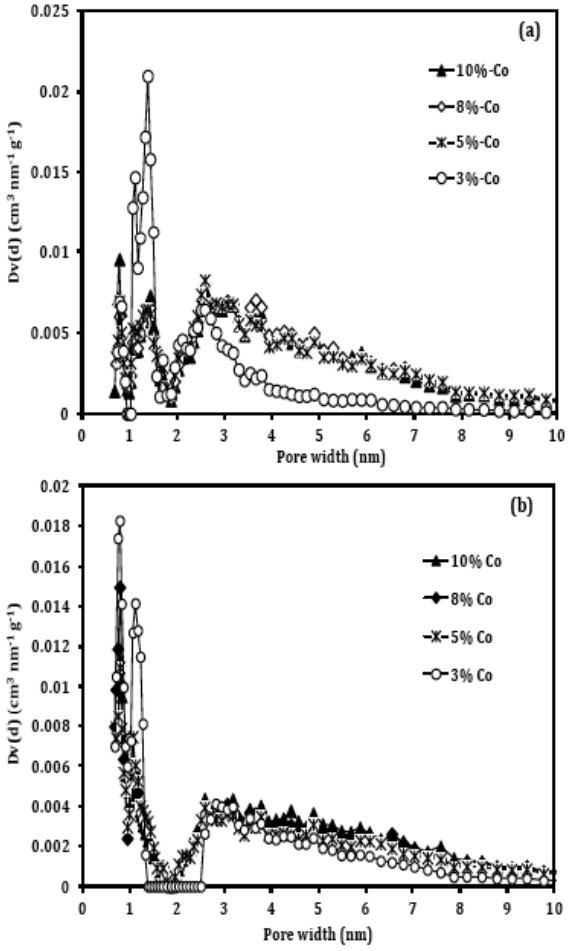

Figure 8: PSD of MTES-X % Co calcined at **a**) 400 °C and **b**) 600 °C.

Obviously, the constant content (3 wt%) cobalt doping process has no effect on the uniform incorporation of organic template. On the other hand, this process improved the thermal stability for the whole xerogel network comparing with the non-doped xerogel and provides an enhanced beneficial structural stability[8]. These micropore results strongly suggest that a cobalt-doped methylated microporous silica xerogels were successfully achieved in the present study by sol-gel method, although some supermicroporosity was observed. In addition to that, the narrow PSD suggests that these xerogels can be used as precursor materials for molecular sieve silica applications. In a field such as gas separation involving large molecules and small diffusing molecules; these materials with supermicropores may facilitate the transport of gas molecules towards narrower pores of the silica membranes. In fact the actual values of the pore width interval of the unsupported cobalt-doped methylated microporous silica may differ somehow from the supported one as well as the actual separation behavior.

3.5. Gas Permeance of the Tubular Hydrophobic Membranes

Based on the results obtained in the aforementioned, Hyd-Si membrane (M1 membrane) and Hyd-Co-Si with 3%-Co (M2 membrane) were prepared by coating on inside γ-Al_2O_3/α-Al_2O_3 supports under normal conditions. Membranes performance was characterized by means of single gas permeation in order to determine the main gas transport mechanism. The permeanceat ∆P=2 bar for both modified and unmodified material, shows a decreasing trend as a result of increasing temperature for all measured gases. For example, H_2 permeance of membrane M1 decreases from 9E-08 to 8E-08 $mol.m^{-2}.s^{-1}.pa^{-1}$ (from 25°C to 150°C). This result is a consequence of the morphology of the final membrane. Figure **9** displays the permselectivity for the probing molecules. The trend is clear in the permselectivity difference between the both membranes. This can be related to the lower number of defects or pinholes of M2 compared with M1.

M2 shows higher selectivity compared with M1 due to the fact that its permselectivity exceed the Knudsen values, and also it has a lower number of defects in the separation layer. The only exception is that M2 shows lower selectivity or exactly Knudsen selectivity for H_2/He. This selectivity is approximately constant with increasing temperature. Both membranes show high

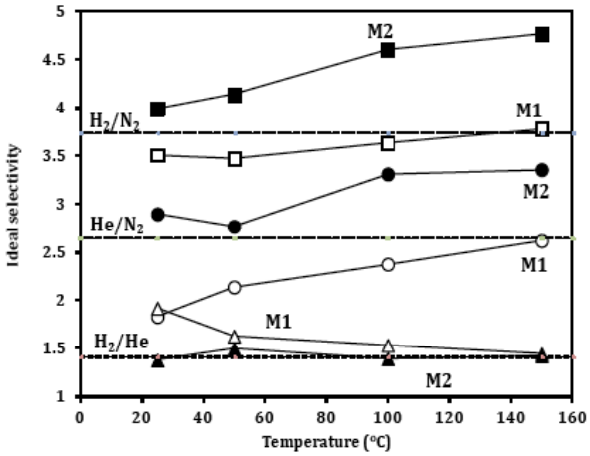

Figure 9: Selectivity of M1 (hollow symbols) and M2 (solid symbols). Dashed lines represent Knudsen selectivity (∆ P = 2 bar).

selectivity with increasing temperature, however, M1 selectivity is approximately on the boundary of Knudsen values. At low temperature, M1 selectivity is lower than the Knudsen values which can be attributed to the influence of viscous flow. Besides, the surface diffusion effect cause that permselectivity results exceed or are on the boundary of the Knudsen values. The reason of low permselectivitiy values is related with the type of support used for the membrane preparation. Low selectivity was also reported using the same type of support for the preparation of carbon molecular sieve supported membranes where the presence of defects avoided observing the characteristic molecular sieving mechanism of carbon molecular sieve membranes [60].The influence of the support in the final membrane properties is discussed at the end of this section. Although the obtained results indicate that these membranes are nondefect-free, the novel silica material can be used in the preparation of silica membranes for gas separation. In a previous work, we demonstrated the lower microporosity achieved after Co incorporation into the Hyd-Si material [8]. This explains the higher separation properties of M1 comparing to M2 membrane. The use of support with more microporous part could be the way to improve a selectivity of the membrane. The Knudsen permeance is given by eq. 1

$$Q = \frac{\varepsilon d_P}{\tau L}\left(\frac{8}{9\pi MRT}\right)^{\frac{1}{2}} \quad (1)$$

where Q is the permeance ($mol.m^{-2}.s^{-1}.Pa^{-1}$), ε the porosity, dp the pore diameter (m), τ the tortuosity, L the membrane thickness (m), R the gas constant

(8.314 J mol^{-1} K^{-1}), T the temperature (K), and M the molecular weight (kg mol^{-1}). The Knudsen diffusion equation predicts that gas permeance will have an inverse square root dependency on both the molecular weight and temperature. The permeance data are plotted vs. the inverse square root of the molecular weight at different temperatures for M1 and M2 in Figure **10**. A good fit to linear regression is obtained (r^2 = 0.917 to 0.993) for M1 and (r^2 = 0.997 to 0.999) for M2. This indicates that the main transport is Knudsen mechanism and this is what was expected [61]. Moreover, the permeance data are plotted vs. the inverse square root of the temperature, (data not shown) evidenced the temperature influence on the whole transport mechanism of the membrane [60].

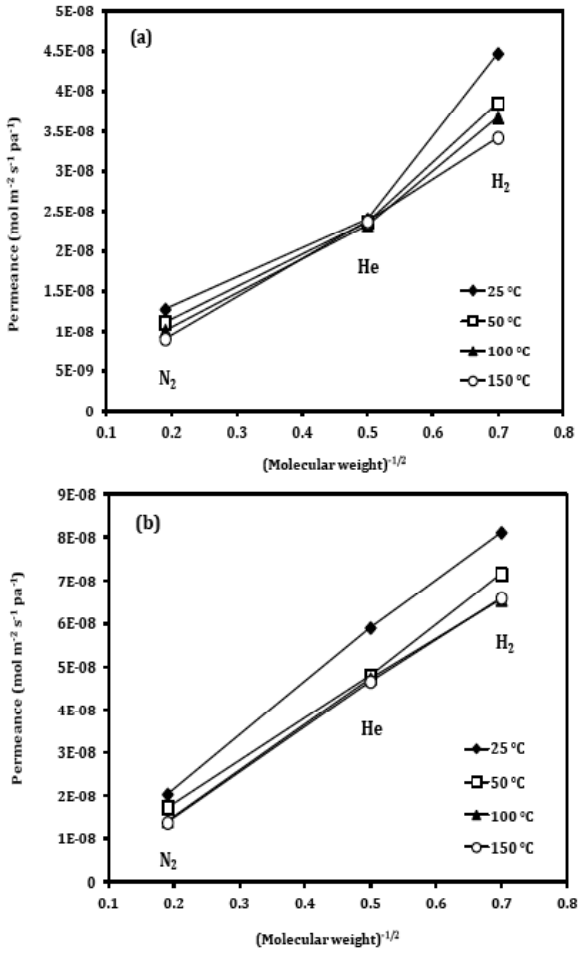

Figure 10: Gas permeance vs. molecular weight $^{-1/2}$ for different gases **a**) M1 and **b**) M2 (Δ P = 2 bar).

In addition to that, the apparent activation energy can be calculated from fitting the experimental data to an Arrhenius equation (2).

$$Q = Q_0 \exp\left(\frac{-E_a}{RT}\right) \quad (2)$$

Where Q is the gas permeance, Q_0 the pre-exponential factor ($mol.m^{-2}.s^{-1}.Pa^{-1}$), Ea the apparent activation energy (KJ mol^{-1}), R the gas constant and T the absolute temperature (K). The fitting results and associated *Ea* are listed in Table **5** together with some data on silica/modified silica membranes that have been prepared by sol-gel and reported elsewhere [50, 62, 63].

The increase of permeability with increasing temperature leads to negative activation energies; therefore, the gas transport is not controlled by activation mechanism. This indicates compatibility with several transport mechanism such as viscous, Knudsen or surface flow, except from molecular sieving mechanism that is unable to describe the experimental results [64]. A similar trend was reported for carbon molecular sieves membranes coated onthe same type of support. Briceño *et al*, also reported negative values of Activation energy for a carbon molecular sieve supported membrane due to the presence of defects[60]. After coating with PDSM it was possible to reduce the effect of viscous flow by some defects undetected by visual inspection. These negative values of *Ea* can be obtained if the gas molecules and pore wall interaction are varied by changes in surface polarity and pore size diameter. The same trend was reported for carbon membrane and microporous silica membrane [60, 62]. Subsequently, the possible hypotheses for the obtained results concerning the permeation of M1 and M2 are:

- The membrane support has a significant effect on the whole transport mechanism due to the way of support modification and membrane preparation that do not lead to highly microporous silica membranes.
- The possible mechanisms are viscous flow, Knudsen diffusion and surface diffusion and/or adsorption.

The support performance can be governed by Knudsen and viscous flow, while the surface diffusion is almost associated to the temperature effect on the microporous domain. The cohabitation of more than one mechanism to govern gas transport was reported elsewhere [60, 65]. In some cases, especially at low temperature, the gas adsorption and diffusion can exist with the predominance for adsorption as reported for nanoporous carbon membranes [66]. Generally, it can be observed that the hydrophobic membranes prepared by that way seem to not be strict microporous

Table 5: Apparent Activation Energies for M1 and M2 at (ΔP= 2 bar)

Probe Molecule		Activation Energy (Ea) kJ/mol		
	He	H_2	N_2	Ref.
M1	-0.13	-2.03	-2.69	
M2	-1.70	-1.71	-.3.29	
Co-SiO_2 (dry conditions)	9.5	–	-5	[50]
SiO_2	–	-3.52	-3.41	[62]
SiO_2	1.7: 4.0*	-1.3: 2.9*	–	[63]

*When more values were presented in a single study, the lowest and the highest one are reported in Table 5.

membranes with Knudsen or molecular sieving properties. Thus, the transport properties obtained would correspond more likely to a transition flow, which occurs when viscous flow and Knudsen diffusion both play a role [64]. However, as first approach, for the novel supported silica membrane presented in this study, we can conclude that the cobalt-doping within the hybrid silica material leads to better membrane performance compared with the non-doped silica membrane, regarding the selectivity and the permeation data that were obtained, in the case of preparation under normal conditions. Moreover, it is considered as simple and cheap way for support modification as well. It should be taken into account the fact that the support plays an important role in the final properties of the membrane, the new material can works in different supports for different needs in gas separation. Recently, Barma *et al.* reported the importance of the support structure in the fabrication of defect free membranes. The quality of the support determines the final performance of silica membranes [67].

4. CONCLUSIONS

Novel organic templated silica xerogels with improved thermal stability were prepared by the sol-gel technique.Metal-doping process improves the thermal properties of the silica matrix which is attributed to the strong framework based on the formation of Si-O-Co linkages. The presented results shows that the thermal stability of the cobalt-doped organic templated silica xerogels was enhanced up to a range of ~ 500-600 °C in oxidizing atmosphere, regardless the MTES content, compared with the non-doped organic templated silica xerogel as reported in the literature. Increasing the calcination temperature from 400 to 600 ºC led to textural changes such as a decrease in the BET area and micropore area and volume. Calcination at 600 °C resulted in samples with similar textural for cobalt content from 5 to 10% wt., suggesting that the cobalt particles were homogeneously dispersed in the silica matrix and opposed to the silica structure collapse. The doping process had no significant effect on the incorporation of the organic template within the silica matrix. The cobalt-doped methylated microporous silica xerogels exhibited trend toward micropores formation along with some supermicroporosity was observed.

Because of the large pore size of the support, preparation under normal conditions led to non defect-free membranes which have an effect on the gas permeation. In that later case, the gas transport in the membranes is governed by the coexistence of more than one mechanism, such as Knudsen and viscous flows, which are related to the mesoporous part of the structure as a consequence of low quality support, while surface diffusion is closely related to the effect of temperature on the microporous domain. Thus, such kind of reported highly thermally stable and microporous tubular silica membrane (novel hydrophobic cobalt-doped silica membrane) with selectivity that exceed Knudsen or on the boundary of Knudsen values could be a good candidate among existing membrane materials for separation process. To that respect, the separation of hydrogen from larger molecules such as hydrocarbons could be more favorable with the membrane investigated in this work; however the type of application must consider the improvement of the support. The results obtained demonstrate the potential of high thermally stable materials that can be precursor materials for molecular sieve silica membranes applications.

ACKNOWLEDGMENTS

Hany Hassan El-Feky acknowledges ‘‘Departament d’ Economia i Coneixement’’ de la ‘‘Generalitat de

Catalunya'' and its department of Support to Universities and Research (SUR del DEC), together with Fons Social Europeu (FSE) for funding. The doctorate programme in Nanoscience and Nanotechnology and Universitat Rovira i Virgili are also acknowledged for research facilities.

REFERENCES

[1] Liang L, Gan Q, Nancarrow P. Composite ionic liquid and polymer membranes for gas separation at elevated temperatures. Journal of Membrane Science. 2014; 450: 407-17. http://dx.doi.org/10.1016/j.memsci.2013.09.033

[2] Chua ML, Shao L, Low BT, Xiao Y, Chung T-S. Polyetheramine–polyhedral oligomeric silsesquioxane organic–inorganic hybrid membranes for CO2/H2 and CO2/N2 separation. Journal of Membrane Science. 2011; 385–386: 40-8. http://dx.doi.org/10.1016/j.memsci.2011.09.008

[3] Zhuang G-L, Wey M-Y, Tseng H-H. The density and crystallinity properties of PPO-silica mixed-matrix membranes produced via the in situ sol-gel method for H2/CO2 separation. II: Effect of thermal annealing treatment. Chem Eng Res Des. 2015; 104: 319-32. http://dx.doi.org/10.1016/j.cherd.2015.08.020

[4] Lu GQ, Diniz da Costa JC, Duke M, Giessler S, Socolow R, Williams RH, et al. Inorganic membranes for hydrogen production and purification: A critical review and perspective. J Colloid Interface Sci. 2007; 314(2): 589-603. http://dx.doi.org/10.1016/j.jcis.2007.05.067

[5] Barelli L, Bidini G, Gallorini F, Servili S. Hydrogen production through sorption-enhanced steam methane reforming and membrane technology: A review. Energy. 2008; 33(4): 554-70. http://dx.doi.org/10.1016/j.energy.2007.10.018

[6] Liu L, Wang DK, Martens DL, Smart S, Diniz da Costa JC. Binary gas mixture and hydrothermal stability investigation of cobalt silica membranes. Journal of Membrane Science. 2015; 493: 470-7. http://dx.doi.org/10.1016/j.memsci.2015.06.058

[7] Zhang X-L, Yamada H, Saito T, Kai T, Murakami K, Nakashima M, et al. Development of hydrogen-selective triphenylmethoxysilane-derived silica membranes with tailored pore size by chemical vapor deposition. Journal of Membrane Science. 2016; 499: 28-35. http://dx.doi.org/10.1016/j.memsci.2015.09.025

[8] El-Feky HH, Brice-o K, Jardim EdO, Silvestre-Albero J, Gumí T. Novel silica membrane material for molecular sieve applications. Microporous Mesoporous Mater. 2013; 179(0): 22-9. http://dx.doi.org/10.1016/j.micromeso.2013.04.029

[9] Wei Q, Ding Y-L, Nie Z-R, Liu X-G, Li Q-Y. Wettability, pore structure and performance of perfluorodecyl-modified silica membranes. Journal of Membrane Science. 2014; 466: 114-22. http://dx.doi.org/10.1016/j.memsci.2014.04.036

[10] Paradis GG, Shanahan DP, Kreiter R, van Veen HM, Castricum HL, Nijmeijer A, et al. From hydrophilic to hydrophobic HybSi® membranes: A change of affinity and applicability. Journal of Membrane Science. 2013; 428: 157-62. http://dx.doi.org/10.1016/j.memsci.2012.10.006

[11] Khatib SJ, Oyama ST. Silica membranes for hydrogen separation prepared by chemical vapor deposition (CVD). Sep Purif Technol. 2013; 111: 20-42. http://dx.doi.org/10.1016/j.seppur.2013.03.032

[12] Castricum HL, Sah A, Kreiter R, Blank DHA, Vente JF, ten Elshof JE. Hydrothermally stable molecular separation membranes from organically linked silica. J Mater Chem. 2008; 18(18): 2150-8. http://dx.doi.org/10.1039/b801972j

[13] Yacou C, Smart S, Diniz da Costa JoC. Long term performance cobalt oxide silica membrane module for high temperature H2 separation. Energy & Environmental Science. 2012; 5(2): 5820-32. http://dx.doi.org/10.1039/c2ee03247c

[14] Ren X, Kanezashi M, Nagasawa H, Tsuru T. Plasma-assisted multi-layered coating towards improved gas permeation properties for organosilica membranes. RSC Advances. 2015; 5(74): 59837-44. http://dx.doi.org/10.1039/C5RA08052E

[15] Hench LL, West JK. The sol-gel process. Chem Rev (Washington, DC, US). 1990; 90(1): 33-72. http://dx.doi.org/10.1021/cr00099a003

[16] S. Sakka. Handbook of sol-gel science and technology : processing, characterization, and applications, Kluwer Academic Publishers, Dordrecht, 2005.

[17] C.J. Brinker, Scherer GW. Sol-gel science : the physics and chemistry of sol-gel processing: Academic Press, Boston; 1990.

[18] Diniz da Costa JC, Lu GQ, Rudolph V, Lin YS. Novel molecular sieve silica (MSS) membranes: characterisation and permeation of single-step and two-step sol–gel membranes. Journal of Membrane Science. 2002; 198(1): 9-21. http://dx.doi.org/10.1016/S0376-7388(01)00565-8

[19] Duke MC, Diniz da Costa JC, Lu GQ, Petch M, Gray P. Carbonised template molecular sieve silica membranes in fuel processing systems: permeation, hydrostability and regeneration. Journal of Membrane Science. 2004; 241(2): 325-33. http://dx.doi.org/10.1016/j.memsci.2004.06.004

[20] Smart S, Vente JF, Diniz da Costa JC. High temperature H2/CO2 separation using cobalt oxide silica membranes. Int J Hydroygen Energy. 2012; 37(17): 12700-7. http://dx.doi.org/10.1016/j.ijhydene.2012.06.031

[21] Elferink WJ, Nair BN, de Vos RM, Keizer K, Verweij H. Sol–gel synthesis and characterization of microporous silica membranes: II. Tailor-making porosity. J Colloid Interface Sci. 1996; 180(1): 127-34. http://dx.doi.org/10.1006/jcis.1996.0282

[22] Mu-oz-Aguado M-J, Gregorkiewitz M. Sol–gel synthesis of microporous amorphous silica from purely inorganic precursors. J Colloid Interface Sci. 1997; 185(2): 459-65. http://dx.doi.org/10.1006/jcis.1996.4564

[23] Nair BN, Elferink WJ, Keizer K, Verweij H. Sol–gel synthesis and characterization of microporous silica membranes I: SAXS study on the growth of polymeric structures. J Colloid Interface Sci. 1996; 178(2): 565-70. http://dx.doi.org/10.1006/jcis.1996.0152

[24] Tsai C-Y, Tam S-Y, Lu Y, Brinker CJ. Dual-layer asymmetric microporous silica membranes. Journal of Membrane Science. 2000; 169(2): 255-68. http://dx.doi.org/10.1016/S0376-7388(99)00343-9

[25] Raman NK, Anderson MT, Brinker CJ. Template-based approaches to the preparation of amorphous, Nanoporous Silicas. Chem Mater. 1996; 8(8): 1682-701. http://dx.doi.org/10.1021/cm960138+

[26] Giessler S, Diniz da Costa JC, Lu GQ. Hydrophobicity of templated silica xerogels for molecular sieving applications. J Nanosci Nanotechnol. 2001; 1(3): 331-6. http://dx.doi.org/10.1166/jnn.2001.037

[27] Wei Q, Wang Y-L, Nie Z-R, Yu C-X, Li Q-Y, Zou J-X, et al. Facile synthesis of hydrophobic microporous silica membranes and their resistance to humid atmosphere.

Microporous Mesoporous Mater. 2008; 111(1–3): 97-103. http://dx.doi.org/10.1016/j.micromeso.2007.07.016

[28] Diniz da Costa JC, Lu GQ, Rudolph V. Characterisation of templated xerogels for molecular sieve application. Colloids Surf, A. 2001; 179(2–3): 243-51. http://dx.doi.org/10.1016/S0927-7757(00)00644-0

[29] Giessler S, Jordan L, Diniz da Costa JC, Lu GQ. Performance of hydrophobic and hydrophilic silica membrane reactors for the water gas shift reaction. Sep Purif Technol. 2003; 32(1–3): 255-64. http://dx.doi.org/10.1016/S1383-5866(03)00069-8

[30] Kusakabe K, Sakamoto S, Saie T, Morooka S. Pore structure of silica membranes formed by a sol–gel technique using tetraethoxysilane and alkyltriethoxysilanes. Sep Purif Technol. 1999; 16(2): 139-46. http://dx.doi.org/10.1016/S1383-5866(98)00120-8

[31] Lu Y, Cao GZ, Kale RP, Delattre L, Brinker CJ, Lopezl GP. Controlling the porosity of microporous silica by sol-gel processing using an organic template approach. Mat Res Soc Symp Proc. 1996; 435: 271-5. http://dx.doi.org/10.1557/PROC-435-271

[32] de Vos RM, Maier WF, Verweij H. Hydrophobic silica membranes for gas separation. Journal of Membrane Science. 1999; 158(1–2): 277-88. http://dx.doi.org/10.1016/S0376-7388(99)00035-6

[33] Giessler S, Duke MC, Diniz da Costa JC, Lu GQ. Hydrothermal Stability of Modified Silica Membranes for Gas Separation. DG Wood 6th World Congress of Chemical Engineering. 2001: 1-10.

[34] Raman NK, Brinker CJ. Organic "template" approach to molecular sieving silica membranes. Journal of Membrane Science. 1995; 105(3): 273-9. http://dx.doi.org/10.1016/0376-7388(95)00067-M

[35] Igi R, Yoshioka T, Ikuhara YH, Iwamoto Y, Tsuru T. Characterization of Co-doped silica for improved hydrothermal stability and application to hydrogen separation membranes at high temperatures. J Am Ceram Soc. 2008; 91(9): 2975-81. http://dx.doi.org/10.1111/j.1551-2916.2008.02563.x

[36] Battersby S, Duke MC, Liu S, Rudolph V, Diniz da Costa JC. Metal doped silica membrane reactor: Operational effects of reaction and permeation for the water gas shift reaction. Journal of Membrane Science. 2008; 316(1–2): 46-52. http://dx.doi.org/10.1016/j.memsci.2007.11.021

[37] Kanezashi M, Asaeda M. Hydrogen permeation characteristics and stability of Ni-doped silica membranes in steam at high temperature. Journal of Membrane Science. 2006; 271(1–2): 86-93. http://dx.doi.org/10.1016/j.memsci.2005.07.011

[38] Boffa V, ten Elshof JE, Garcia R, Blank DHA. Microporous niobia–silica membranes: Influence of sol composition and structure on gas transport properties. Microporous Mesoporous Mater. 2009; 118(1–3): 202-9. http://dx.doi.org/10.1016/j.micromeso.2008.08.038

[39] Petersen J, Matsuda M, Haraya K. Capillary carbon molecular sieve membranes derived from Kapton for high temperature gas separation. Journal of Membrane Science. 1997; 131(1–2): 85-94. http://dx.doi.org/10.1016/S0376-7388(97)00041-0

[40] Fotou GP, Lin YS, Pratsinis SE. Hydrothermal stability of pure and modified microporous silica membranes. J Mater Sci. 1995; 30(11): 2803-8. English. http://dx.doi.org/10.1007/BF00349647

[41] de Vos RM, Verweij H. Improved performance of silica membranes for gas separation. Journal of Membrane Science. 1998; 143(1–2): 37-51. http://dx.doi.org/10.1016/S0376-7388(97)00334-7

[42] Sinkó K, Szabó G, Zrínyi M. Liquid-phase synthesis of cobalt oxide nanoparticles. J Nanosci Nanotechnol. 2011; 11(5): 4127-35. http://dx.doi.org/10.1166/jnn.2011.3875

[43] Mansour SAA. Spectrothermal studies on the decomposition course of cobalt oxysalts Part II. Cobalt nitrate hexahydrate. Mater Chem Phys. 1994; 36(3–4): 317-23. http://dx.doi.org/10.1016/0254-0584(94)90048-5

[44] Kojima K, Taguchi H, Matsuda J. Optical and magnetic properties of cobalt(2+) ions in dried and heated silica gels prepared by the sol-gel process. J Phys Chem. 1991 1991/10/01; 95(20): 7595-8.

[45] Esposito S, Turco M, Ramis G, Bagnasco G, Pernice P, Pagliuca C, et al. Cobalt–silicon mixed oxide nanocomposites by modified sol–gel method. J Solid State Chem. 2007; 180(12): 3341-50. http://dx.doi.org/10.1016/j.jssc.2007.09.032

[46] Ortega-Zarzosa G, Araujo-Andrade C, Compeán-Jasso ME, Martínez JR, Ruiz F. Cobalt oxide/silica xerogels powders: X-ray diffraction, infrared and visible absorption studies. J Sol-Gel Sci Technol. 2002; 24(1): 23-9. http://dx.doi.org/10.1023/A:1015105414916

[47] Olejniczak Z, Łęczka M, Cholewa-Kowalska K, Wojtach K, Rokita M, Mozgawa W. 29Si MAS NMR and FTIR study of inorganic–organic hybrid gels. J Mol Struct. 2005; 744–747(0): 465-71. http://dx.doi.org/10.1016/j.molstruc.2004.11.069

[48] Qi H, Han J, Xu N. Effect of calcination temperature on carbon dioxide separation properties of a novel microporous hybrid silica membrane. Journal of Membrane Science. 2011; 382(1–2): 231-7. http://dx.doi.org/10.1016/j.memsci.2011.08.013

[49] Duran A, Serna C, Fornes V, Fernandez Navarro JM. Structural considerations about SiO2 glasses prepared by sol-gel. J Non-Cryst Solids. 1986; 82(1–3): 69-77. http://dx.doi.org/10.1016/0022-3093(86)90112-2

[50] Uhlmann D, Liu S, Ladewig BP, Diniz da Costa JC. Cobalt-doped silica membranes for gas separation. Journal of Membrane Science. 2009; 326(2): 316-21. http://dx.doi.org/10.1016/j.memsci.2008.10.015

[51] Brunauer S, Emmett PH, Teller E. Adsorption of gases in multimolecular layers. J Am Chem Soc. 1938; 60(2): 309-19. http://dx.doi.org/10.1021/ja01269a023

[52] de Boer JH, Lippens BC, Linsen BG, Broekhoff JCP, van den Heuvel A, Osinga TJ. Thet-curve of multimolecular N2-adsorption. J Colloid Interface Sci. 1966; 21(4): 405-14. http://dx.doi.org/10.1016/0095-8522(66)90006-7

[53] Neimark AV, Ravikovitch PI. Capillary condensation in MMS and pore structure characterization. Microporous Mesoporous Mater. 2001; 44–45(0): 697-707. http://dx.doi.org/10.1016/S1387-1811(01)00251-7

[54] Sing KSW, Everett DH, Haul RAW, Moscou L, Pierotti RA, Rouquerol J, et al. Reporting physisorption data for gas solid systems with special reference to the determination of surface-area and porosity (recommendations 1984). Pure Appl Chem. 1985; 57(4): 603-19. http://dx.doi.org/10.1351/pac198557040603

[55] Nunes CD, Pires J, Carvalho AP, Calhorda MJ, Ferreira P. Synthesis and characterisation of organo-silica hydrophobic clay heterostructures for volatile organic compounds removal. Microporous Mesoporous Mater. 2008; 111(1–3): 612-9. http://dx.doi.org/10.1016/j.micromeso.2007.09.008

[56] Rouquerol F, Rouquerol J, Sing K. Adsorption by powders and porous solids, principles, methodology and applications, Academic Press, London, 1999.

[57] Castricum HL, Sah A, Mittelmeijer-Hazeleger MC, Huiskes C, Elshof JEt. Microporous structure and enhanced hydrophobicity in methylated SiO2 for molecular separation. J Mater Chem. 2007; 17(15): 1509-17. http://dx.doi.org/10.1039/b610311a

[58] 58. Fahrenholtz WG, Smith DM, Hua D-W. Formation of microporous silica gels from a modified silicon alkoxide. I. Base-catalyzed gels. Journal of Non-Crystalline Solids. 1992; 144(0): 45-52.

[59] 59. Darmawan A, Smart S, Julbe A, Diniz da Costa JC. Iron oxide silica derived from sol-gel synthesis. Materials. 2011; 4(2): 448-56. http://dx.doi.org/10.3390/ma4020448

[60] Briceño K, Iulianelli A, Montané D, Garcia-Valls R, Basile A. Carbon molecular sieve membranes supported on non-modified ceramic tubes for hydrogen separation in membrane reactors. Int J Hydrogen Energy. 2012; 37(18): 13536-44. http://dx.doi.org/10.1016/j.ijhydene.2012.06.069

[61] Lee D, Zhang L, Oyama ST, Niu S, Saraf RF. Synthesis, characterization, and gas permeation properties of a hydrogen permeable silica membrane supported on porous alumina. Journal of Membrane Science. 2004; 231(1–2): 117-26.

[62] Richard V, Favre E, Tondeur D, Nijmeijer A. Experimental study of hydrogen, carbon dioxide and nitrogen permeation through a microporous silica membrane. Chem Eng J (Lausanne). 2001; 84(3): 593-8. http://dx.doi.org/10.1016/S1385-8947(01)00173-5

[63] Yoshioka T, Nakanishi E, Tsuru T, Asaeda M. Experimental studies of gas permeation through microporous silica membranes. AIChE J. 2001; 47(9): 2052-63. http://dx.doi.org/10.1002/aic.690470916

[64] Burggraaf AJ, Cot L. Fundamentals of inorganic membrane science and technology Amsterdam, New York: Elsevier; 1996.

[65] Wang D, Teo WK, Li K. Permeation of H_2, N_2, CH_4, C_2H_6, and C_3H_8 through asymmetric polyetherimide hollow-fiber membranes. J Appl Polym Sci. 2002; 86(3): 698-702. http://dx.doi.org/10.1002/app.10966

[66] Liu BS, Wang N, He F, Chu JX. Separation performance of nanoporous carbon membranes fabricated by catalytic decomposition of CH_4using Ni/Polyamideimide templates. Ind Eng Chem Res. 2008; 47(6): 1896-902. http://dx.doi.org/10.1021/ie071161f

[67] Sanjib Barma BM. Synthesis and characterization of ordered mesoporous silica membrane: role of porous supports and gas permeation study. Microporous and Mesoporous Materials. 2015; 210: 10-9. http://dx.doi.org/10.1016/j.micromeso.2015.02.011

Received on 09-11-2015 Accepted on 22-12-2015 Published on 01-01-2016

http://dx.doi.org/10.15379/2410-1869.2015.02.02.09